UAV-Enabled Accompanying Coverage for Hybrid Satellite-UAV-Terrestrial Maritime Communications

Xiangling Li*, Wei Feng*, Yunfei Chen†, Cheng-Xiang Wang‡§, Ning Ge*
*Beijing National Research Center for Information Science and Technology, Tsinghua University, Beijing 100084, China
‡National Mobile Communications Research Laboratory,
School of Information Science and Engineering, Southeast University, Nanjing 210096, China
§Purple Mountain Laboratories, Nanjing 211111, China
†School of Engineering, University of Warwick, Coventry CV4 7AL, U.K.
E-mail: lingjlu@yeah.net, fengwei@tsinghua.edu.cn, Yunfei.Chen@warwick.ac.uk,
chxwang@seu.edu.cn, gening@tsinghua.edu.cn

***Abstract*—Despite of constantly-developing satellites and terrestrial fifth generation (5G) communications, there is still a large gap for maritime broadband coverage. In this paper, we explore the potential gain of unmanned aerial vehicles (UAVs) for maritime communications. A hybrid satellite-UAV-terrestrial network is considered, where the UAV is employed to offer an accompanying coverage for mobile ships. We optimize both the trajectory and transmit power of UAV to maximize the minimum of ship's achievable rate. Different from previous studies, we consider a typical composite channel model containing both large-scale and small-scale fading, to cope with the practical propagation environment. Moreover, we assume only the large-scale channel state information (CSI) is known for optimization, because the dynamic small-scale fading cannot be obtained before UAV's flight, whereas the large-scale CSI can be estimated according to the position information of ships. Under this context, an optimization problem is formulated, subject to constraints on UAV's kinematics and communication limitation. We solve the problem which is proved to be non-convex by problem decomposition, successive convex optimization and bisection searching tools. Simulation results have corroborated the superiority of the proposed accompanying coverage of UAV.**

I. Introduction

UAV has shown a considerable promise for coverage enhancement. Specially, different projects have been initiated to exploit UAVs to provide on demand broadband service for rural and poorly covered areas, such as the Facebook Drone project and the FP7 SUNNY project.

The key difference of UAV-enabled communications from traditional ones lies in UAV's controllable mobility. When a static UAV is used hovering above the coverage area, the benefits mainly depend on the UAV's altitude [1]. When a mobile UAV is employed, its trajectory should be carefully designed [2]–[4]. The majority of existing studies have simplified this issue by considering some simple cases, e.g., the circular trajectory [2], [3]. Besides, energy efficiency was considered for trajectory optimization in [5] and [6]. For mobile users, the UAV trajectory should cater to the positions of mobile users, resulting in an emerging accompanying coverage technologies [7], [8]. In [7] and [8], the ergodic achievable rate was maximized by adjusting the fixed-wing UAV heading.

In this paper, we investigate the potential gain of UAV in the maritime scenario where the broadband coverage is still an open issue [9]. For maritime communications, the channel model is much different from traditional ones [10]–[12]. To be practical, both large-scale and small-scale fading should be considered as that in [2]. The corresponding CSI has great impact on both trajectory design and communication strategy optimization [3]–[6]. When the simplest free space path loss model is assumed, it is relatively easy to obtain some theoretical results [3]–[6], which however can only provide a rough lower performance bound for realistic systems. When it comes to the more complicated composite maritime channel model, the accurate CSI cannot be assumed to be known, because it is difficult to acquire the small-scale CSI before UAV's flight. Thus, only large-scale CSI can be used for trajectory and communication strategy optimization, which unfortunately remains elusive to the best of the authors' knowledge.

In this paper, we discuss the optimal design of UAV trajectory and transmit power with large-scale CSI condition. Note that satellites and terrestrial onshore-base stations (BSs) already exist for maritime communications. We thus focus on a hybrid satellite-UAV-terrestrial network, where the UAV is employed to offer an accompanying coverage for mobile ships. The UAV shares spectrum with existing satellites and achieves backhaul service from the onshore BS. We observe that it is easy to obtain the position information of mobile ships, according to, e.g., information from the standard automatic identification system (AIS). Therefore, we assume only the large-scale CSI is known for optimization, which varies slowly and highly depends on the positions, and thus can be obtained before UAV's flight. Under this context, an optimization problem is formulated, subject to constraints on UAV's kinematics, backhaul, tolerable leakage interference, and total communication energy. The problem is proved to be non-convex. We solve it by problem decomposition, successive convex optimization, and bisection searching tools. Simulation results will show the superiority of the proposed accompanying coverage.

II. System Model

We consider a hybrid satellite-UAV-terrestrial maritime communication network, as shown in Fig. 1. To mitigate

978-1-7281-0660-1/19/$31.00

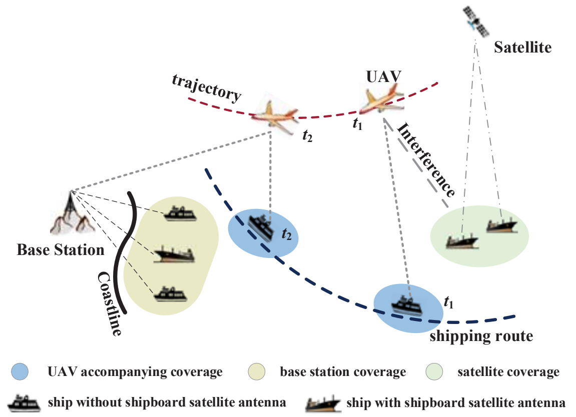

Fig. 1. Illustration of a hybrid satellite-UAV-terrestrial maritime communication network, where grey dotted lines denote wireless communication links.

coverage holes of onshore BSs and satellites, the UAV is deployed to accommodate the communication requirement of mobile ships. The UAV is employed as an aerial platform of BS, which has the abilities of inter-cell handover, resource allocation, etc. The UAV waits near the onshore BS while not being used.

The spectrum is shared between UAV and satellite to deal with spectrum scarcity problem. This leads to the interference from UAV to the ships served by satellites. To mitigate the interference, UAV trajectory and transmit power are adjusted. Moreover, onshore BS provides wireless backhaul for UAV. We assume there is no interference between backhaul and access side of UAV.

A typical composite channel with both large-scale and small-scale fading is considered. We assume that UAV and mobile ships are equipped with single antenna. Let $h_{a,i,t}$ and $d_{a,i,t}$ denote the channel and distance between the a-th transmitter and the i-th receiver at time t, respectively. We have $h_{a,i,t} = L_{a,i,t}^{-1/2}\tilde{h}_{a,i,t}$, where $L_{a,i,t}$ denotes the path loss and $\tilde{h}_{a,i,t}$ denotes Rician fading. The path loss model is

$$L_{a,i,t}\,(\mathrm{dB}) = A_0 + 10\varsigma \log 10\left(\frac{d_{a,i,t}}{d_0}\right) + X_{a,i,t} \tag{1}$$

where A_0 is the path loss at the reference distance d_0, ς is the path-loss exponent, and $X_{a,i,t} \in \mathcal{N}(0,\sigma_X)$ [12]. Rician fading can be expressed as $\tilde{h}_{a,i,t} = \sqrt{\frac{K}{1+K}} + \sqrt{\frac{1}{1+K}}g_{a,i,t}$, where $g_{a,i,t} \in \mathcal{CN}(0,1)$ and K is the Rician factor. The path loss and Rician fading are categorized into the large-scale and small-scale CSI, respectively. The path loss is related to the transmission distance. On the ocean, the ship's position information can be obtained. Thus, we assume that the large-scale CSI can be obtained before UAV's flight.

III. UAV-Enabled Accompanying Coverage

In this section, we describe the details of UAV-enabled accompanying coverage. Firstly, under the composite channel model, we formulate the optimization problem of the UAV trajectory and transmit power. Then, by utilizing the obtainable large-scale CSI, an iterative algorithm is proposed to solve the optimization problem.

A. Problem Formulation

Let Γ_s and Γ_a denote the sets of onshore BSs and UAVs, respectively. Let Ω_a and Ω_o denote the sets of the ships served by UAVs and satellites, respectively. Let T_0 be the travel time during which a UAV serves a mobile ship. The positions of UAV and the ship served by UAV at time t are denoted as $\mathbf{c}_{a,t} = [x_{a,t}, y_{a,t}, z_{a,t}]^T$ and $\mathbf{c}_{i,t} = [x_{i,t}, y_{i,t}, z_{i,t}]^T$, respectively, where $a \in \Gamma_a$ and $i \in \Omega_a$. Let us assume that an onshore BS provides wireless backhaul for the UAV during T_0. The onshore BS is located at $(0,\ 0,\ z_{s,t})$, where $s \in \Gamma_s$. The ergodic achievable rate $R_{a,i,t}$ between the a-th transmitter and the i-th receiver at time t can be expressed as

$$R_{a,i,t} = \mathbf{E}\left\{\log_2\left[1 + \frac{P_{a,t}G_aG_i|h_{a,i,t}|^2}{\sigma^2}\right]\right\} \tag{2}$$

where $P_{a,t}$ denotes the transmit power and σ^2 denotes the white Gaussian noise power, and G_a/G_i denote the gain of the transmitting/receiving antenna, and $\mathbf{E}\{\cdot\}$ denotes the expectation operator, and $|\cdot|$ indicates the absolute value of a scalar. Assuming that the large-scale CSI is obtainable, the expectation is taken over Rician fading.

The optimization problem can be formulated as

$$\max_{P_{a,t},\mathbf{c}_{a,t},\mathbf{v}_{a,t},\mathbf{a}_{a,t}} \quad \min_{t} \quad R_{a,i,t} \tag{3a}$$
$$\text{subject to} \quad \mathbf{v}_{a,t} = \dot{\mathbf{c}}_{a,t} \tag{3b}$$
$$\mathbf{a}_{a,t} = \ddot{\mathbf{c}}_{a,t} \tag{3c}$$
$$\|\mathbf{v}_{a,t}\|_2^2 \geq v_{\min}^2 \tag{3d}$$
$$\|\mathbf{v}_{a,t}\|_2^2 \leq v_{\max}^2 \tag{3e}$$
$$\|\mathbf{a}_{a,t}\|_2^2 \leq a_{\max}^2 \tag{3f}$$
$$z_{\min} \leq z_{a,t} \leq z_{\max} \tag{3g}$$
$$0 \leq P_{a,t} \leq P_{\max} \tag{3h}$$
$$\sum\nolimits_{t\in\Lambda_1} P_{a,t}\Delta t \leq E_0 \tag{3i}$$
$$R_{a,i,t} \leq R_{s,a,t} \tag{3j}$$
$$\mathbf{E}\left[P_{a,t}G_aG_j|h_{a,j,t}|^2\right] \leq I_0, j \in \Omega_o' \tag{3k}$$

where the minimum ergodic achievable rate during T_0 is maximized by optimizing UAV trajectory, transmit power, velocities, and accelerations. The travel time T_0 is discretized into T time slots with a step size Δt. The trajectory and transmit power are adjusted in each time slot. The details about the constraints are given as follows.

$\mathbf{v}_{a,t}$ and $\mathbf{a}_{a,t}$ denote the velocity and the acceleration of UAV. According to the definition, we have $\mathbf{v}_{a,t} = \dot{\mathbf{c}}_{a,t}$ and $\mathbf{a}_{a,t} = \ddot{\mathbf{c}}_{a,t}$, while $v_{\max}$, $v_{\min}$ and $a_{\max}$ denote the maximum and minimum velocity, and the maximum acceleration, respectively. $z_{\max}$ and $z_{\min}$ denote the maximum and minimum altitude, respectively, $z_{\min}$ is used to guarantee the light-of-sight (LOS) link, and $z_{\max}$ is set according to the air traffic control. The communication energy is provided by the battery. The energy consumption during T_0 is limited. So, we have $\sum_{t=1}^{T} P_{a,t}\Delta t \leq E_0$, where

E_0 denotes energy consumption during T_0. $P_{\max}$ denotes maximum transmit power. Due to wireless backhaul, the achievable rate is limited in the BS-to-UAV link. Thus, we have $R_{a,i,t} \leq R_{s,a,t}$. Let $\Omega'_{o,t}$ be the set of ships served by satellites and interfered by UAV, and $|\Omega'_{o,t}| = M_t$. To limit the interference, an interference temperature limitation I_0 is used.

Different from the algorithms in [7] and [8], UAV trajectory and transmit power are jointly optimized. Moreover, UAV's velocity and acceleration are used as constraints. More importantly, we use the composite channel model and the expectation of achievable rates is taken over Rician fading, which are different from the algorithms in [3]–[6].

B. An Iterative Solution

To solve the optimization problem in (3), we determine the concavity and monotonicity of the ergodic achievable rate $R_{a,i,t}$. The result is shown as follows.

Theorem 1: The ergodic achievable rate $R_{a,i,t}$ in (2), where the expectation is taken over the Rician fading, is strictly concave and monotonically increasing with the average signal-to-noise ratio (SNR) $a_{a,i,t} = P_{a,t} G_a G_i L_{a,i,t}^{-1} \sigma^{-2}$.

Proof: The proof is given in Appendix A. ■

Because $R_{a,i,t}$ is a concave function, the optimization problem in (3) is non-convex. To solve the problem in (3), by using the monotonicity, the objective function in (3a) is rewritten as

$$\max_{P_{a,t}, \mathbf{c}_{a,t}, \mathbf{v}_{a,t}, \mathbf{a}_{a,t}} \ \min_{t} \ P_{a,t} G_a G_i L_{a,i,t}^{-1} \sigma^{-2} \tag{4}$$

and the constraint in (3j) is expressed as

$$P_{a,t} G_a G_i L_{a,i,t}^{-1} \sigma^{-2} \leq P_{s,t} G_s G_a L_{s,a,t}^{-1} \sigma^{-2} \tag{5}$$

where $P_{s,t}$ denotes the transmit power of the onshore BS.

The problem in (3) is still difficult because of the derivatives in (3b) and (3c). Based on the first-order and second-order Taylor approximations, the constraints in (3b) and (3c) are rewritten as $\mathbf{v}_{a,t+1} \approx \mathbf{v}_{a,t} + \mathbf{a}_{a,t} \Delta t$ and $\mathbf{c}_{a,t+1} \approx \mathbf{c}_{a,t} + \mathbf{v}_{a,t} \Delta t + \frac{1}{2} \mathbf{a}_{a,t} \Delta t^2$. Let $\Delta \mathbf{v}_t = \mathbf{v}_{a,t+1} - (\mathbf{v}_{a,t} + \mathbf{a}_{a,t} \Delta t)$ and $\Delta \mathbf{c}_t = \mathbf{c}_{a,t+1} - \left(\mathbf{c}_{a,t} + \mathbf{v}_{a,t} \Delta t + \frac{1}{2} \mathbf{a}_{a,t} \Delta t^2\right)$. Since $g_{a,j,t} \in \mathcal{CN}(0,1)$, $\mathbf{E}\left[P_{a,t} G_a G_j |h_{a,j,t}|^2\right] = P_{a,t} G_a G_j L_{a,j,t}^{-1}$. Let $\mathrm{Q} = \min_t P_{a,t} G_a G_i L_{a,i,t}^{-1} \sigma^{-2}$. According to the above analysis, the problem in (3) can be rewritten as

$$\max_{P_{a,t}, \mathbf{c}_{a,t}, \mathbf{v}_{a,t}, \mathbf{a}_{a,t}, Q} \ Q \tag{6a}$$

$$\text{subject to} \ (3d), (3e), (3f), (3g), (3h), (3i), (5)$$

$$|\Delta v_{w,t}| \leq \Delta v_0 \tag{6b}$$

$$|\Delta c_{w,t}| \leq \Delta c_0 \tag{6c}$$

$$Q \leq P_{a,t} G_a G_i L_{a,i,t}^{-1} \sigma^{-2} \tag{6d}$$

$$P_{a,t} G_a G_j L_{a,j,t}^{-1} \leq I_0 \tag{6e}$$

where $\Delta v_{w,t}$ and $\Delta c_{w,t}$ denote the w-th element in $\Delta \mathbf{v}_t$ and $\Delta \mathbf{c}_t$, and $w \in \{1,2,3\}$. Δv_0 and Δc_0 are set to be small values.

In (5), (6d) and (6e), $P_{a,t}$ and $\mathbf{c}_{a,t}$ are in the numerator and denominator of fractions. To make the analysis easy, according to the monotonicity of power functions, we have

$$(B_{s,t} P_{s,t})^{\frac{2}{\varsigma}} \|\mathbf{c}_{a,t} - \mathbf{c}_{i,t}\|_2^2 - (B_{i,t} P_{a,t})^{\frac{2}{\varsigma}} \|\mathbf{c}_{a,t} - \mathbf{c}_{s,t}\|_2^2 \geq 0 \tag{7}$$

$$Q^{\frac{2}{\varsigma}} \|\mathbf{c}_{a,t} - \mathbf{c}_{i,t}\|_2^2 \leq (B_{i,t} P_{a,t})^{\frac{2}{\varsigma}} \tag{8}$$

$$I_0^{\frac{2}{\varsigma}} \left\|\mathbf{c}_{a,t} - \mathbf{c}_{j,t}\right\|_2^2 \geq (B_{j,t} P_{a,t})^{\frac{2}{\varsigma}} \tag{9}$$

where $B_{i,t} = G_a G_i d_0^{\varsigma} \sigma^{-2} 10^{-\frac{A_0 + X_{a,i,t}}{10}}$, $B_{s,t} = G_s G_a d_0^{\varsigma} \sigma^{-2} 10^{-\frac{A_0 + X_{s,a,t}}{10}}$ and $B_{j,t} = G_a G_j d_0^{\varsigma} \sigma^{-2} 10^{-\frac{A_0 + X_{a,j,t}}{10}}$. One sees that $\|\mathbf{v}_{a,t}\|_2^2$, $\|\mathbf{a}_{a,t}\|_2^2$, $\|\mathbf{c}_{a,t} - \mathbf{c}_{i,t}\|_2^2$ and $\left\|\mathbf{c}_{a,t} - \mathbf{c}_{j,t}\right\|_2^2$ are convex functions. Besides, by analyzing the second-order derivatives, the equality in (7) is a concave constraint if $B_{s,t} P_{s,t} > B_{i,t} P_{a,t}$. Then, due to the constraints in (3d), (7) and (9), the problem in (6) is still non-convex. To make the problem in (6) more tractable, we obtain Lemma 1.

Lemma 1: For any given $\mathbf{v}_{a,t}^r$ and $\mathbf{c}_{a,t}^r$, we have

$$\left\|\mathbf{v}_{a,t}^r\right\|_2^2 + 2 \mathbf{v}_{a,t}^{r\,T} (\mathbf{v}_{a,t} - \mathbf{v}_{a,t}^r) \geq v_{\min}^2 \tag{10}$$

$$(B_{s,t} P_{s,t})^{\frac{2}{\varsigma}} f_{a,i,t} \geq (B_{i,t} P_{a,t})^{\frac{2}{\varsigma}} \|\mathbf{c}_{a,t} - \mathbf{c}_{s,t}\|_2^2 \tag{11}$$

$$I_0^{\frac{2}{\varsigma}} f_{a,j,t} \geq (B_{j,t} P_{a,t})^{\frac{2}{\varsigma}} \tag{12}$$

where

$$f_{a,i,t} = \left\|\mathbf{c}_{a,t}^r - \mathbf{c}_{i,t}\right\|_2^2 + 2(\mathbf{c}_{a,t}^r - \mathbf{c}_{i,t})^T (\mathbf{c}_{a,t} - \mathbf{c}_{a,t}^r). \tag{13}$$

Proof: As a convex function is lower-bounded by its first-order Taylor expansion [13], by combining (3d), (7) and (9), the lemma is proved. ■

According to Lemma 1, the problem in (6) can be iteratively solved by utilizing the successive convex optimization. In the l-th iteration, by using $\mathbf{v}_{a,t}^{l-1}$ and $\mathbf{c}_{a,t}^{l-1}$ obtained in the $(l-1)$-th iteration, we have the following optimization problem

$$\max_{P_{a,t}^l, \mathbf{c}_{a,t}^l, \mathbf{v}_{a,t}^l, \mathbf{a}_{a,t}^l, Q^l} \ Q^l \tag{14a}$$

$$\text{subject to} \ \left|\Delta v_{w,t}^l\right| \leq \Delta v_0 \tag{14b}$$

$$\left|\Delta c_{w,t}^l\right| \leq \Delta c_0 \tag{14c}$$

$$\left\|\mathbf{v}_{a,t}^l\right\|_2^2 \leq v_{\max}^2 \tag{14d}$$

$$\left\|\mathbf{a}_{a,t}^l\right\|_2^2 \leq a_{\max}^2 \tag{14e}$$

$$z_{\min} \leq z_{a,t}^l \leq z_{\max} \tag{14f}$$

$$0 \leq P_{a,t}^l \leq P_{\max} \tag{14g}$$

$$\sum\nolimits_{t \in \Lambda_1} P_{a,t}^l \Delta t \leq E_0 \tag{14h}$$

$$(Q^l)^{\frac{2}{\varsigma}} \left\|\mathbf{c}_{a,t}^l - \mathbf{c}_{i,t}\right\|_2^2 \leq (B_{i,t} P_{a,t}^l)^{\frac{2}{\varsigma}} \tag{14i}$$

$$\left\|\mathbf{v}_{a,t}^{l-1}\right\|_2^2 + 2 \mathbf{v}_{a,t}^{l-1\,T} (\mathbf{v}_{a,t}^l - \mathbf{v}_{a,t}^{l-1}) \geq v_{\min}^2 \tag{14j}$$

$$(B_{i,t} P_{a,t}^l)^{\frac{2}{\varsigma}} \left\|\mathbf{c}_{a,t}^l - \mathbf{c}_{s,t}\right\|_2^2 \leq (B_{s,t} P_{s,t})^{\frac{2}{\varsigma}} f_{a,i,t}^l \tag{14k}$$

$$(B_{j,t} P_{a,t}^l)^{\frac{2}{\varsigma}} \leq I_0^{\frac{2}{\varsigma}} f_{a,j,t}^l \tag{14l}$$

where $\Delta v^l_{w,t}$ and $\Delta c^l_{w,t}$ are similar to those in (6b) and (6c). $f^l_{a,i,t}$ and $f^l_{a,j,t}$ are obtained by replacing $\mathbf{c}^r_{a,t}$ and $\mathbf{c}_{a,t}$ in (13) with $\mathbf{c}^{l-1}_{a,t}$ and $\mathbf{c}^l_{a,t}$, respectively.

In (14), there exits coupling relationships among Q^l, $P^l_{a,t}$ and $\mathbf{c}^l_{a,t}$ because of multiplication operations. Consequently, we decouple the problem in (14) into two subproblems. First, for given $\mathbf{c}^l_{a,t}$, we optimize $P^l_{a,t}$. Then, for given $P^l_{a,t}$, we optimize $\mathbf{c}^l_{a,t}$. The details are described as follows.

1) transmit power: For given $\mathbf{c}^{l-1}_{a,t}$, set $\mathbf{c}^l_{a,t} = \mathbf{c}^{l-1}_{a,t}$. The problem for optimizing $P^l_{a,t}$ can be expressed as

$$\max_{P^l_{a,t}, Q^l} \quad Q^l \tag{15}$$
$$\text{subject to} \quad (14g), (14h), (14i), (14k), (14l).$$

The problem in (15) is a LP and can be solved with CVX.

2) three-dimensional coordinates, velocities and accelerations: For given $P^l_{a,t}$, $\mathbf{c}^{l-1}_{a,t}$ and $\mathbf{v}^{l-1}_{a,t}$, the problem in (14) can be optimized by solving the following problem

$$\max_{\mathbf{c}^l_{a,t}, \mathbf{v}^l_{a,t}, \mathbf{a}^l_{a,t}, Q^l} \quad Q^l \tag{16}$$
$$\text{subject to} \quad (14b), (14c), (14d), (14e),$$
$$(14f), (14i), (14j), (14k), (14l).$$

To deal with coupling relationships between Q^l and $\mathbf{c}^l_{a,t}$, the bisection method is employed. The problem in (16) is decoupled into a series of convex problems by setting Q^m and solved iteratively. In the m-th iteration, for any fixed point Q^m, with $\mathbf{c}^{l-1}_{a,t}$, $\mathbf{v}^{l-1}_{a,t}$ and $P^l_{a,t}$ obtained by solving the problem in (15), the convex problem can be written as

$$\text{find} \quad \mathbf{c}^m_{a,t}, \mathbf{v}^m_{a,t}, \mathbf{a}^m_{a,t} \tag{17}$$
$$\text{subject to} \quad (14b), (14c), (14d), (14e),$$
$$(14f), (14i), (14j), (14k), (14l).$$

In (17), the superscript l in constraints should be replaced with m except $P^l_{a,t}$, $\mathbf{v}^{l-1}_{a,t}$ and $\mathbf{c}^{l-1}_{a,t}$. The shortest distance between UAV and mobile ship is $z_{\min}$. Given $P^l_{a,t}$, the upper bound of Q^m is $U^0 = P^l_{a,t} B_{i,t} z^{-\varsigma}_{\min}$. The lower bound of Q^m is set to be $L^0 = 0$. In the m-th iteration, set $Q^m = \frac{U^0 + L^0}{2}$. If the problem in (17) is solved, set $L^0 = Q^m$, otherwise set $U^0 = Q^m$. After iterations, the maximum Q^m can be obtained.

IV. Simulation Results and Discussion

In this section, simulation is performed to validate the performance. An onshore BS located at $(0, 0, 100)$ m provides wireless backhaul for a UAV. The UAV begins to serve a ship when the ship moves from the point $(5.0 \times 10^4, 0, 10)$ m to $(6.8 \times 10^4, 0, 10)$ m. $T = 10$ points are uniformly sampled from ship positions and used for simple analysis, denoted as $\mathbf{c}_{i,t} = [x_{i,t}, y_{i,t}, z_{i,t}]^T$. The ship's velocity is denoted as v_i. The ships served by satellites nearest to the UAV and the mobile ship are seriously affected by interference. So without loss of generality, we set $M_t = 1$. The positions of the ships served by satellites and interfered by UAV are $\mathbf{c}_{j,t} = [x_{i,t}, y_{i,t} + (-1)^t \times 8000, z_{i,t}]^T$. The antenna gains of the onshore BS, the UAV, the ships served by satellites and the UAV are set to be 12 dBi, 8 dBi, 8 dBi and 30 dBi. Set the carrier frequency be 5GHz. The path loss is $L_{i,j,t}\,(\text{dB}) = 116.7 + 15\log 10\left(\frac{d_{i,j,t}}{2600}\right) + X_{i,j,t}$, where the standard deviation of $X_{i,j,t}$ is 0.1. The main parameters are shown in Table I. For each experiment, a scene is randomly generated and the small-scale CSI is generated 1000 rounds for obtaining the ergodic achievable rates.

TABLE I
Simulation Parameters.

Symbol	Value	Symbol	Value
$z_{\min}$	2.6 km	$v_{\min}$	30 m/s
$z_{\max}$	5.0 km	$v_{\max}$	60 m/s
v_i	10 m/s	$P_{s,t}$	40 dBm
σ^2	-107 dBm	$a_{\max}$	10 m^2/s

We compare the proposed algorithm with those in [4] and [5], where the whole trajectory was optimized with full CSI. Because it is difficult to achieve small-scale CSI, full CSI could be inaccurate. Our proposed algorithm consider large-scale CSI. To verify the performance gain obtained by using large-scale CSI, we set $I_0 = -40$ dBm and the interference can be ignored in this simulation setup. The transmit power is limited by maximum transmit power, backhaul and total communication energy. Besides, a basic trajectory is used for comparison, based on which UAV flies above the user at the minimum altitude. The transmit power is set to satisfy the constraints. The initial trajectory of UAV is $\mathbf{c}_{a,t} = [x_{i,t}/2, y_{i,t}, z_{\min}]^T$.

The results are shown in Fig. 2, where E_0 is 500 J. When $P_{\max} \leq 30$ dBm, the performance is mainly determined by backhaul and $P_{\max}$. As the existing algorithms ignore $P_{\max}$, we reduce its resulted transmit power to satisfy this constraint. One can see that the performance can be improved with optimization problem subject to the constraint of maximum transmit power. When $P_{\max} \geq 30$ dBm, the performance is mainly determined by backhaul and E_0, which is similar to that in [4]. Our proposed algorithm achieves better performance than that in [4]. To further verify the performance gain obtained by using large-scale CSI, we vary Rician factor K. By decreasing K, our proposed algorithm achieves much better performance than the existing algorithms. One can see that the performance can be improved with large-scale CSI.

An optimized trajectory in the x-y plane is shown in Fig. 3, where $P_{\max} = 40$ dBm, $I_0 = -55$ dBm, $E_0 = 4000$ J, and $K = 31.3$. The optimized trajectory is between the onshore BS and the ship because of the backhaul constraint. Besides, the interference constraint bends the optimized trajectory. The obtained transmit power of UAV $P_{a,t}$ is lower than $P_{\max}$ and satisfies E_0.

V. Conclusions

In this paper, we have investigated the hybrid satellite-UAV-terrestrial maritime communication network. Using only the large-scale CSI, we have jointly designed the trajectory

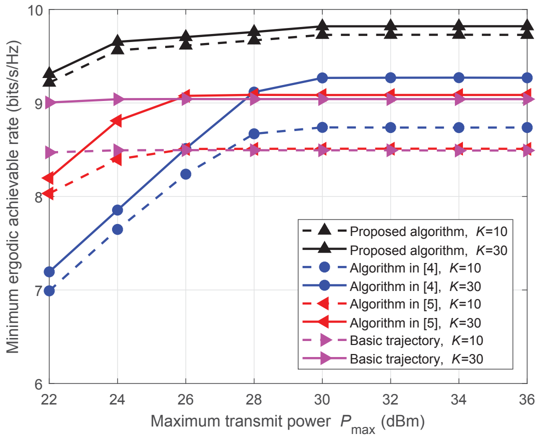

Fig. 2. Comparisons of the minimum ergodic achievable rate.

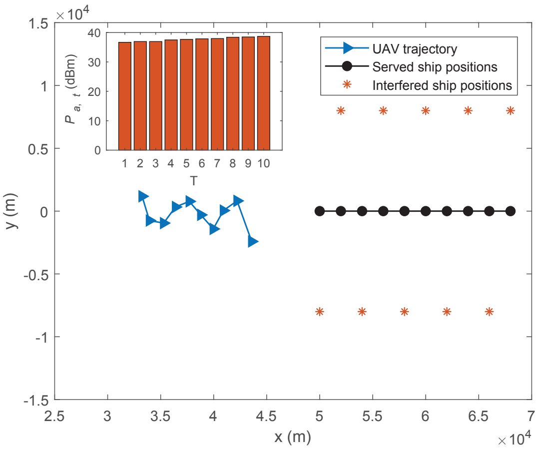

Fig. 3. An optimized trajectory in the x-y plane.

and transmit power of UAV, so as to promote accompanying coverage for mobile ships. To be practical, both constraints in terms of kinematics and communications have been considered in the optimization. Simulation results have shown that it is promising to integrate UAVs into maritime networks using only the large-scale CSI.

VI. Acknowledgment

This work was supported in part by the Beijing Natural science Foundation (L172041), in part by the National Science Foundation of China (61771286, 61701457, 91638205, 61671478), in part by the Fundamental Research Funds for the Central Universities under Grant 2242019R30001, in part by the EU H2020 RISE TESTBED project (Grant No. 734325), and in part by the Beijing Innovation Center for Future Chip.

Appendix A
Proof of Theorem 1

The path loss $L_{a,i,t}$ in (1) can be obtained and the expectation is taken over $g_{a,i,t}$. Since $g_{a,i,t} \in \mathcal{CN}(0,1)$, the average SNR $\mathbf{E}\left\{P_{a,t}G_aG_i|h_{a,i,t}|^2\sigma^{-2}\right\}$ is $a_{a,i,t} = P_{a,t}G_aG_iL_{a,i,t}^{-1}\sigma^{-2}$. Let $b_{a,i,t} = \left|\sqrt{\frac{K}{1+K}} + \sqrt{\frac{1}{1+K}}g_{a,i,t}\right|^2$, which follows a non-central chi-square probability density function with two degrees of freedom, i.e., $f_{b_{a,i,t}}(\gamma) = (1+K)e^{-K}e^{-(1+K)\gamma}I_0\left(2\sqrt{K(1+K)\gamma}\right)$, where $\gamma \geq 0$ and $I_0(\cdot)$ is the zeroth-order modified Bessel function of the first kind [14]. Then, $R_{a,i,t}$ in (2) can be rewritten as $R_{a,i,t} = \log_2 e \int_0^\infty \ln(1+a_{a,i,t}\gamma) f_{b_{a,i,t}}(\gamma)\, d\gamma$. We verify the relationship between $R_{a,i,t}$ and $a_{a,i,t}$ by the first-order and second-order derivatives. The first-order derivative with respect to $a_{a,i,t}$ is

$$\dot{R}_{a,i,t} = \log_2 e \int_0^\infty (1+a_{a,i,t}\gamma)^{-1}\gamma f_{b_{a,i,t}}(\gamma)\, d\gamma. \quad (18)$$

The second-order derivative with respect to $a_{a,i,t}$ is

$$\ddot{R}_{a,i,t} = -\log_2 e \int_0^\infty (1+a_{a,i,t}\gamma)^{-2}\gamma^2 f_{b_{a,i,t}}(\gamma)\, d\gamma. \quad (19)$$

Because $a_{a,i,t} \geq 0$ and $f_{b_{a,i,t}}(\gamma) > 0$, $\dot{R}_{a,i,t} > 0$ and $\ddot{R}_{a,i,t} < 0$ hold. So, $R_{a,i,t}$ is an increasing function of $a_{a,i,t}$ and strictly concave. Thus, the theorem can be proved.

References

[1] Y. Chen, W. Feng, and G. Zheng, "Optimum placement of UAV as relays," *IEEE Commun. Lett.*, vol. 22, no. 2, pp. 248–251, Feb. 2018.

[2] W. Feng, J. Wang, Y. Chen, X. Wang, N. Ge, and J. Lu, "UAV-aided MIMO communications for 5G internet of things," *IEEE Intern. Things. J.*, Oct. 2018.

[3] J. Zhang, Y. Zeng, and R. Zhang, "UAV-enabled radio access network: multi-mode communication and trajectory design," *IEEE Trans. Sign. Proc.*, vol. 66, no. 20, pp. 5269–5284, Oct. 2018.

[4] Y. Zeng, R. Zhang, and T. J. Lim, "Throughput maximization for UAV-enabled mobile relaying systems," *IEEE Trans. Commun.*, vol. 64, no. 12, pp. 4983–4996, Dec. 2016.

[5] Y. Zeng and R. Zhang, "Energy-efficient UAV communication with trajectory optimization," *IEEE Trans. Wireless. Commun.*, vol. 16, no. 6, pp. 3747–3760, Mar. 2017.

[6] D. H. Choi, S. H. Kim, and D. K. Sung, "Energy-efficient maneuvering and communication of a single UAV-based relay," *IEEE Trans. Aero. Elec. Sys.*, vol. 50, no. 3, pp. 2320–2327, Jul. 2014.

[7] P. Zhan, K. Yu, and A. Lee Swindlehurst, "Wireless relay communications with unmanned aerial vehicles: performance and optimization," *IEEE Trans. Aero. Elec. Sys.*, vol. 47, no. 3, pp. 2068–2085, Jul. 2011.

[8] F. Jiang and A. Lee Swindlehurst, "Optimization of UAV heading for the ground-to-air uplink," *IEEE J. Sel. Areas Commun.*, vol. 30, no. 5, pp. 993–1005, Jun. 2012.

[9] C. Liu, W. Feng, T. Wei, and N. Ge, "Fairness-oriented hybrid precoding for massive MIMO maritime downlink systems with large-scale CSIT," *China Communi.*, vol. 15, no. 1, pp. 52–61, Jan. 2018.

[10] C.-X. Wang, J. Bian, J. Sun, W. Zhang, and M. Zhang, "A survey of 5G channel measurements and models," *IEEE Commun. Surveys Tuts.*, vol. 20, no. 4, pp. 3142–3168, 4th Quart., 2018.

[11] S. Wu, C.-X. Wang, H. Aggoune, M. M. Alwakeel, and X. You, "A general 3D non-stationary 5G wireless channel model," *IEEE Trans. Commun.*, vol. 66, no. 7, pp. 3065–3078, Jul. 2018.

[12] D. W. Matolak and R. Sun, "Air-ground channel characterization for unmanned aircraft systems-Part I methods, measurements and models for over-water settings," *IEEE Trans. Veh. Tech.*, vol. 66, no. 1, pp. 4389–4400, Jan. 2017.

[13] S. Boyd and L. Vandenberghe, Convex Optimization, Cambridge, U.K.: Cambridge Univ. Press, 2004.

[14] M. K. Simon and M.-S. Alouini, Digital Communication over Fading Channels, John Wiley & Sons, 2005.